Supporting Information

Active Learning-driven Quantitative Synthesis-Structure-Property Relations for Improving Performance and Revealing Active Sites of Nitrogen-Doped Carbon for the Hydrogen Evolution Reaction

Elvis Ebikade[1,2,#], Yifan Wang[1,2,#], Nicholas Samulewicz[1,2], Bjorn Hasa[1], Dionisios Vlachos[1,2,*]

[1]Catalysis Center for Energy Innovation, University of Delaware, 221 Academy St., Newark, DE 19716, USA

[2]Department of Chemical and Biomolecular Engineering, University of Delaware, 150 Academy St., Newark, DE 19716, USA

*Corresponding author: vlachos@udel.edu

# E.E. and Y.W. contributed equally to this work.

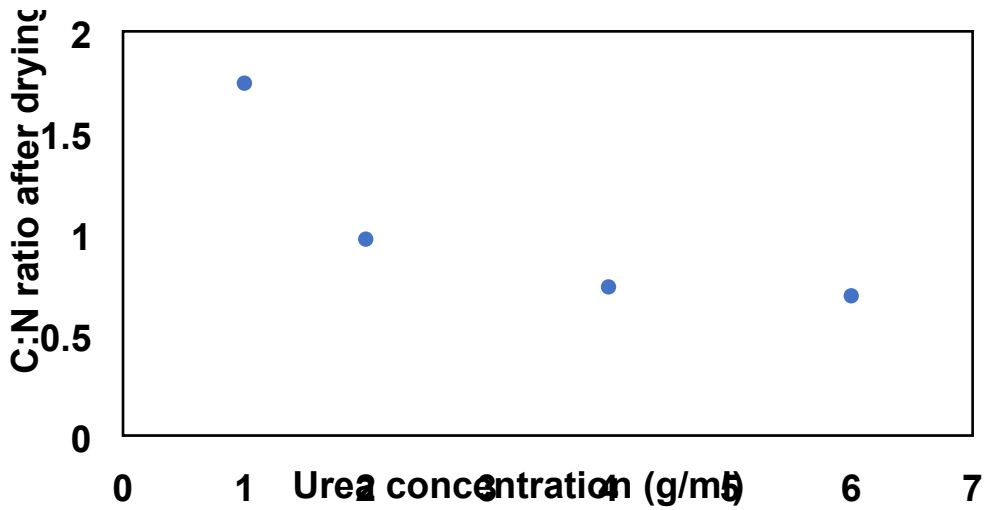

Figure S1. C:N ratio of impregnated carbon precursor after drying.

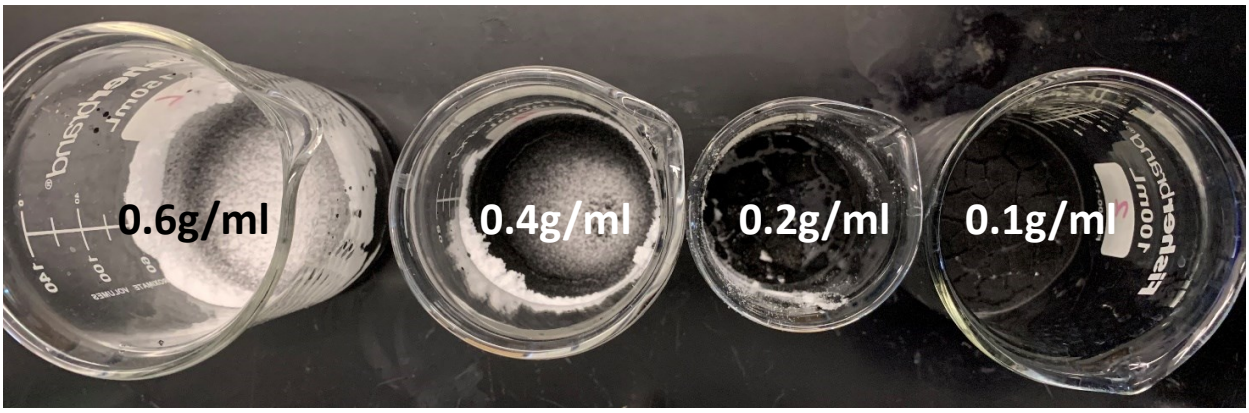

Figure S2. Insoluble urea (white particles) formed after drying impregnated carbon precursor.

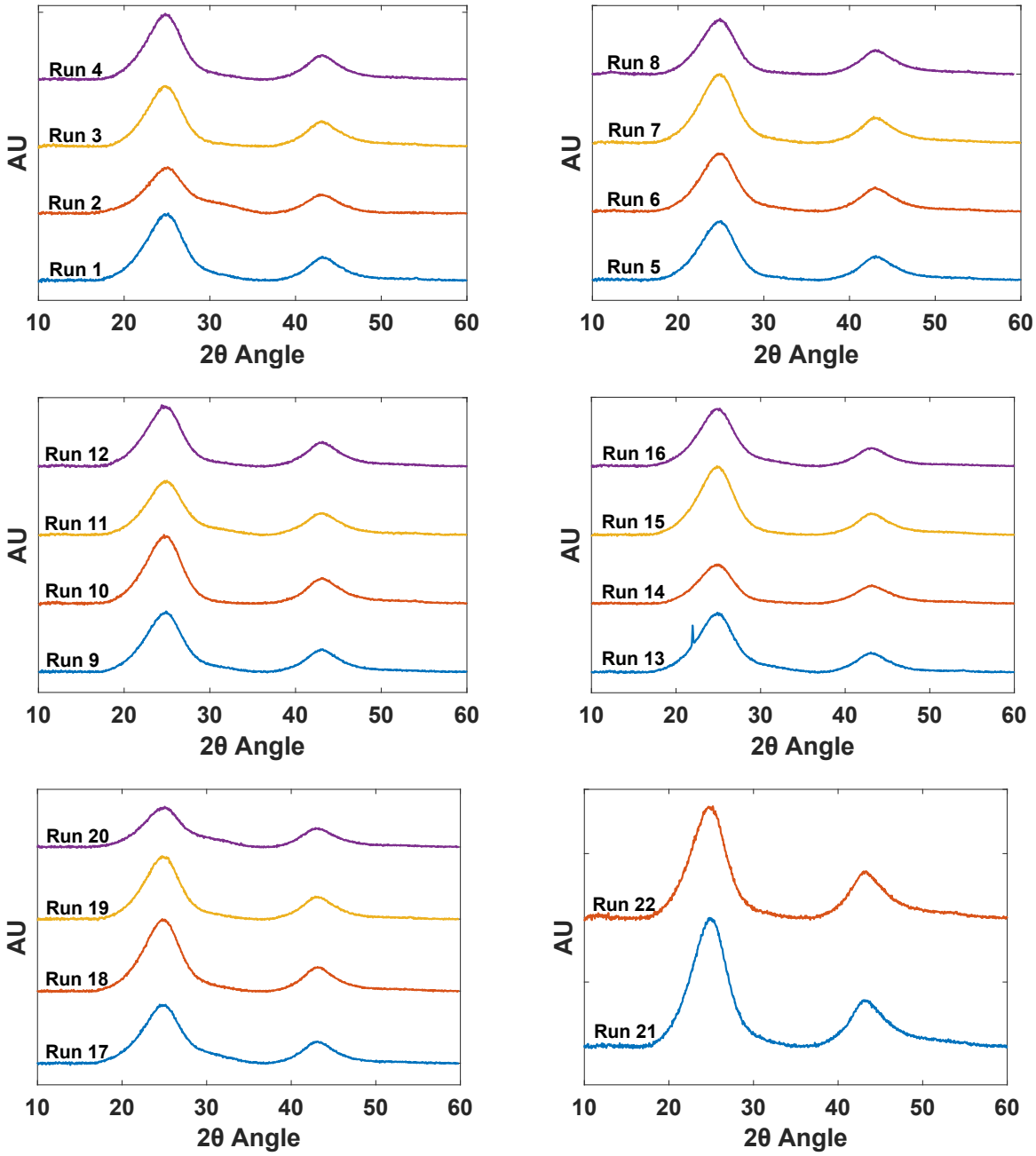

Figure S3. XRD patterns of the synthesized nitrogen doped catalysts.

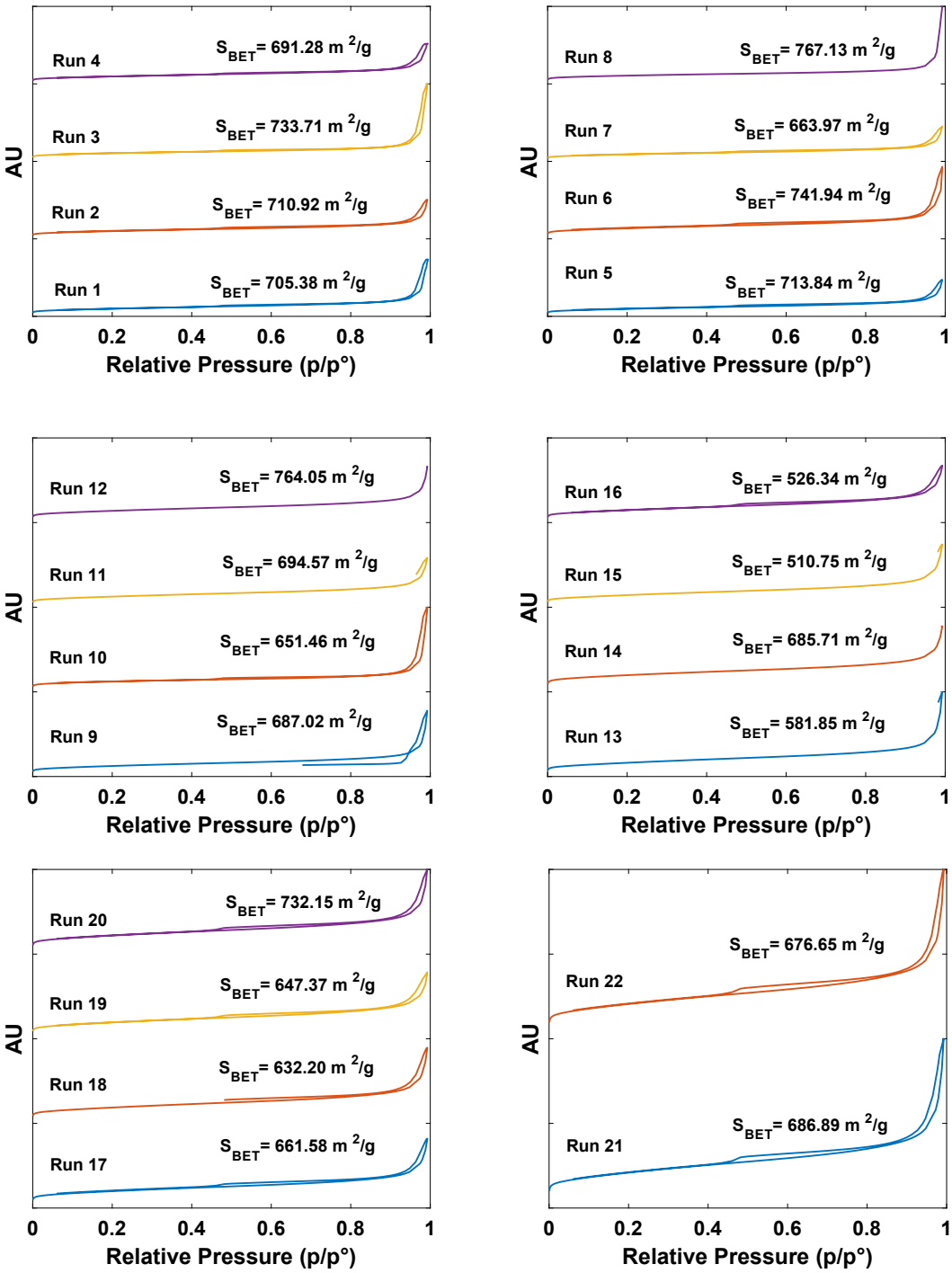

Figure S4. BET N_2 adsorption/desorption isotherms of the synthesized nitrogen doped catalysts.

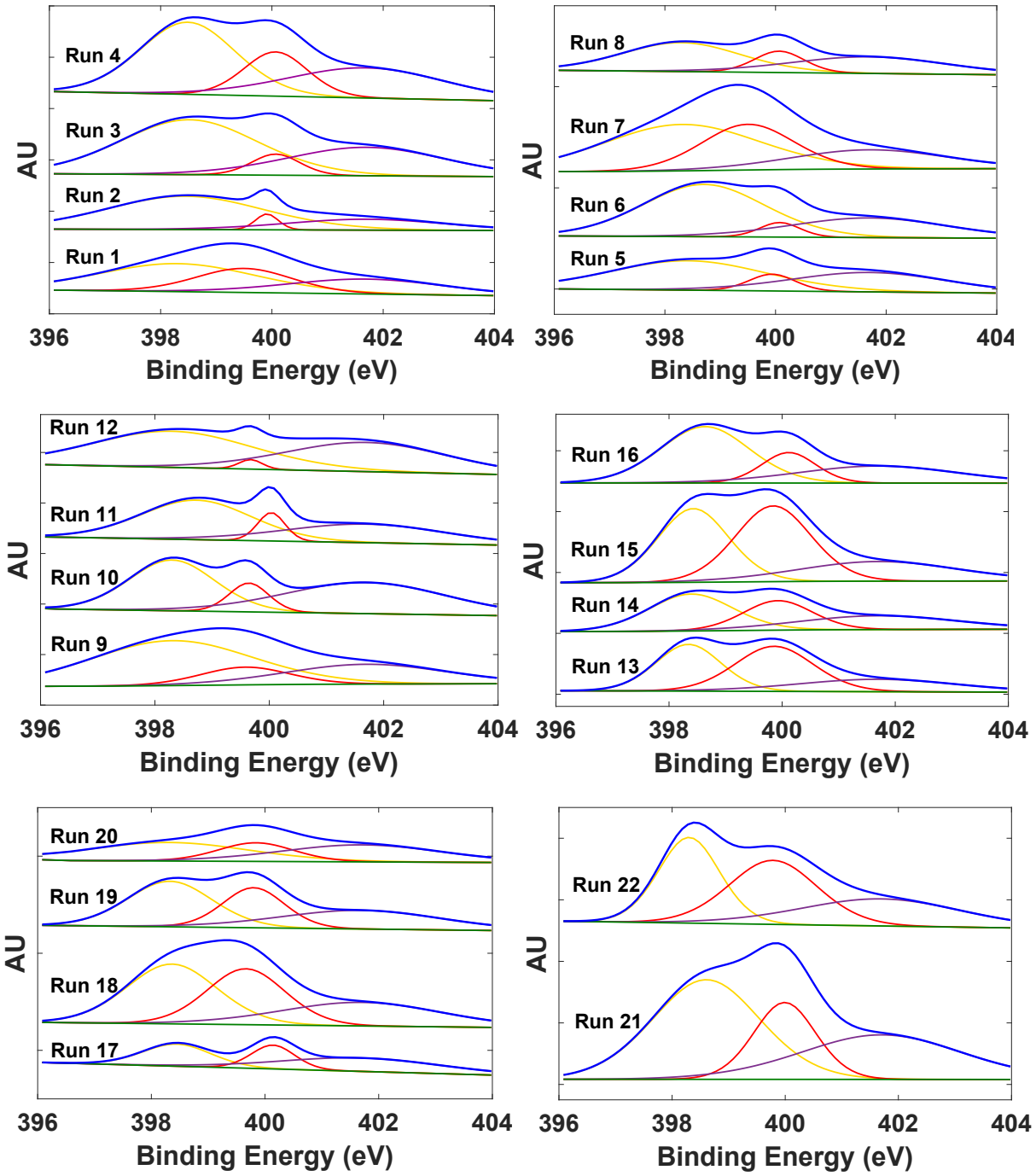

Figure S5. N1s XPS spectra of all synthesized NDCs.

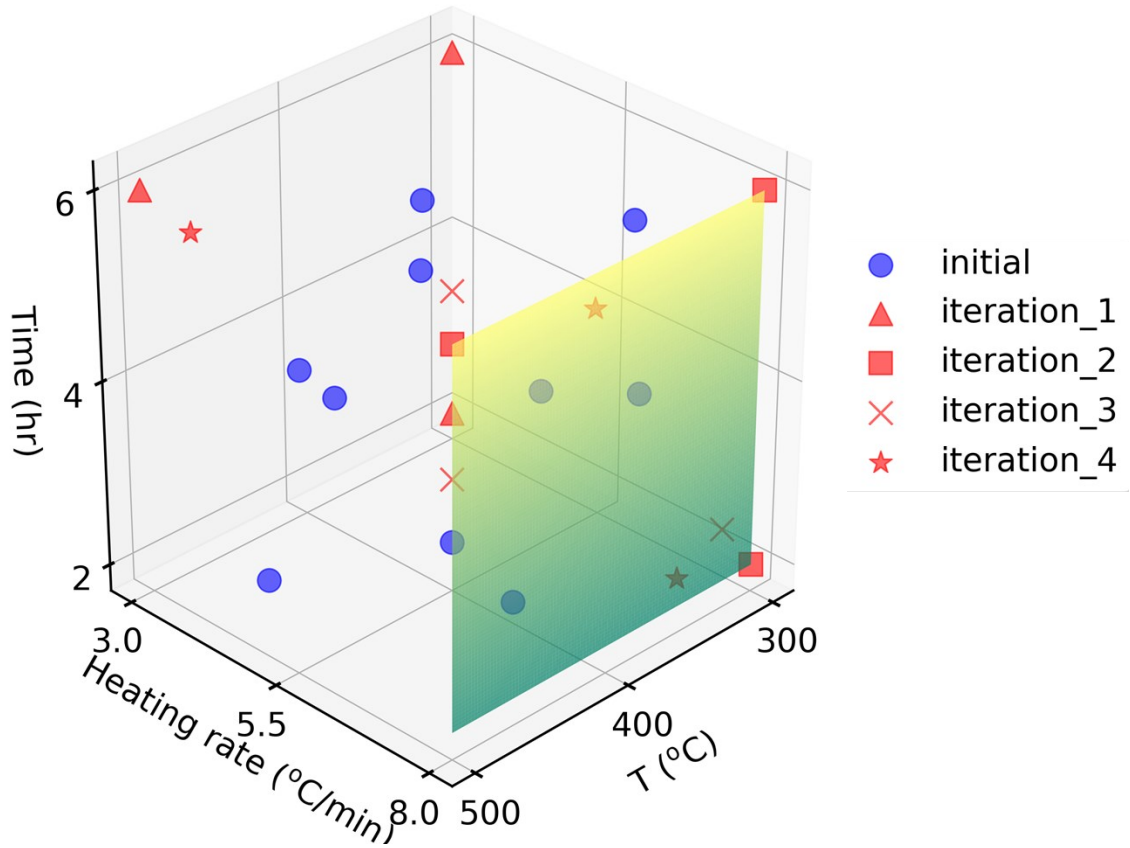

Figure S6. The sampling points, visualized in 3D, consist of 10 initial points using a Latin Hypercube design and 3 points per iteration generated by the Kriging algorithm. The 2D response surface from Figure 5 is shown in green.

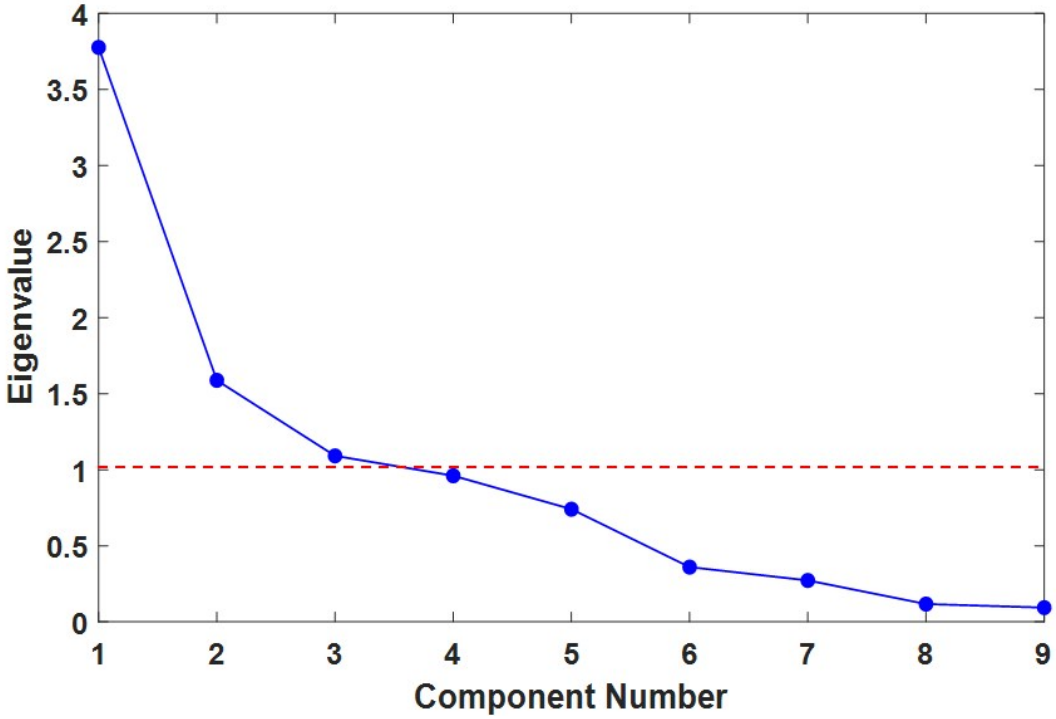

Figure S7. Scree plot of PCA analysis.

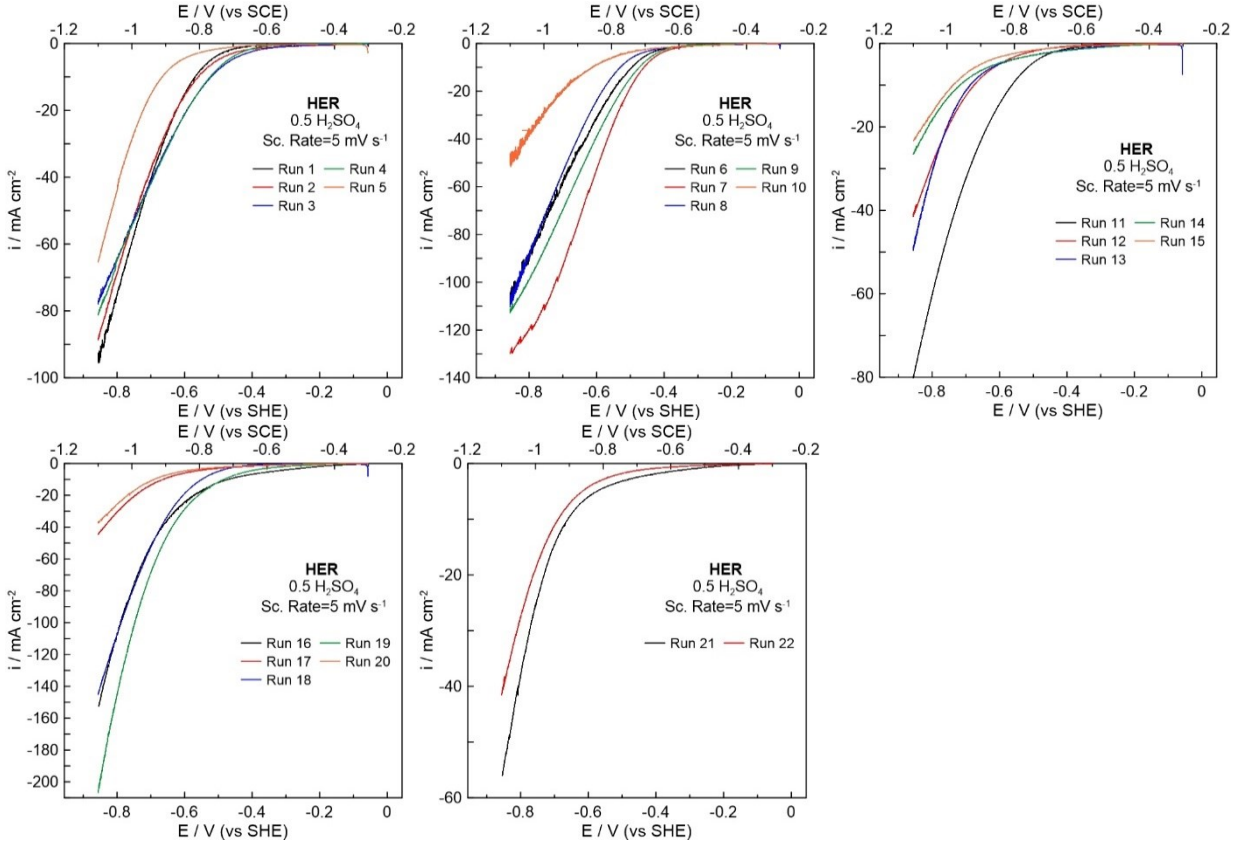

Figure S8. HER polarization curves of the synthesized NDCs.

	Final Temp (°C)	Heat Rate (°C/min)	Hold Time (hr.min)	$N_{content}$ (%)	$N_{Pyridinic}$	$N_{Pyrrolic}$	$N_{Graphitic}$	S_{BET} m²/g	V_m cm³/g	% Crystallinity
1	370	7.75	4.36	1.84	0.97	0.22	0.65	705.38	0.05	77.8
2	490	4.75	2.36	1.17	0.72	0.04	0.41	710.92	0.06	71.2
3	330	5.25	3.24	0.72	0.40	0.10	0.22	733.71	0.10	76.5
4	410	6.75	2.12	1.58	0.69	0.36	0.53	691.28	0.05	76.8
5	450	4.25	4.12	1.30	0.68	0.11	0.51	713.84	0.05	77.5
6	390	3.25	3.00	0.96	0.48	0.14	0.34	741.94	0.10	75.6
7	310	6.25	5.24	1.62	0.79	0.41	0.42	663.97	0.05	78.3
8	470	7.25	3.48	0.77	0.38	0.24	0.15	767.13	0.12	76.4
9	350	3.75	5.00	2.07	1.11	0.34	0.62	687.02	0.06	77.1
10	430	5.75	5.48	2.14	1.01	0.28	0.85	651.46	0.11	79.5
11	300	3.00	2.00	2.40	1.30	0.25	0.85	694.57	0.06	75.1
12	500	3.00	6.00	1.42	0.89	0.09	0.44	764.05	0.07	76.4
13	300	3.00	6.00	1.94	0.97	0.52	0.45	581.15	0.03	76.9
14	500	8.00	6.00	1.03	0.48	0.16	0.39	685.71	0.08	75.2
15	300	8.00	2.00	2.31	0.81	1.01	0.49	510.75	0.03	78.5
16	300	8.00	6.00	2.82	1.53	0.62	0.67	526.34	0.02	76.4
17	490	7.75	4.48	1.53	0.69	0.44	0.4	661.58	0.07	74.1
18	310	3.25	3.55	1.74	0.78	0.51	0.45	632.20	0.05	77.1
19	310	7.75	2.39	1.30	0.69	0.23	0.38	647.37	0.05	77.1
20	479	3.25	5.48	1.25	0.58	0.17	0.50	732.15	0.07	69.0
21	400	7.75	5.48	1.55	0.73	0.34	0.48	686.90	0.06	75.2
22	341	7.75	2.12	1.84	0.82	0.29	0.50	676.65	0.05	73.4

First ten runs are the initial dataset. 3 additional runs added at each iteration. S_{BET} - BET surface area, V_m - micropore volume

Table S1. Summary of NDC N content, individual N type content, surface area, micropore volume, crystallinity and synthesis conditions.

Table S1. HER performance measured in terms of onset potential and maximum current density for the synthesized catalysts.

Run	Onset potential (V *vs* SHE)	i_{max} (mA/cm^2) at -0.88 V *vs* SHE
1	-0.34	-100.0
2	-0.34	-93.0
3	-0.34	-82.0
4	-0.34	-85.4
5	-0.40	-68.8
6	-0.26	-112.2
7	-0.29	-136.6
8	-0.29	-115.5
9	-0.34	-117.8
10	-0.30	-53.7
11	-0.39	-54.6
12	-0.44	-67.8
13	-0.31	-51.6
14	-0.26	-33.5
15	-0.33	-56.4
16	-0.20	-154.0
17	-0.29	-46.6
18	-0.32	-145.0
19	-0.28	-205.5
20	-0.34	-36.2
21	-0.29	-59.5
22	-0.40	-43.5

Table S3. Comparison of the HER performance of our NDC with select metal free catalysts reported in literature in acid media (0.5 M H_2SO_4).

Catalyst	Onset potential (V *vs* SHE)	Ref
Run 16	-0.20	This work
N, P-G-1	-0.29	[1]
N-graphene	-0.33	[1]
p-graphene	-0.37	[1]
B-substituted graphene	-0.38	[2]
borylated defective graphene	-0.42	[2]
Pt/C	-0.03	[3]
NCN - X	(-0.03 ~ - 0.4)	[3]

X = 800°C – 1000°C

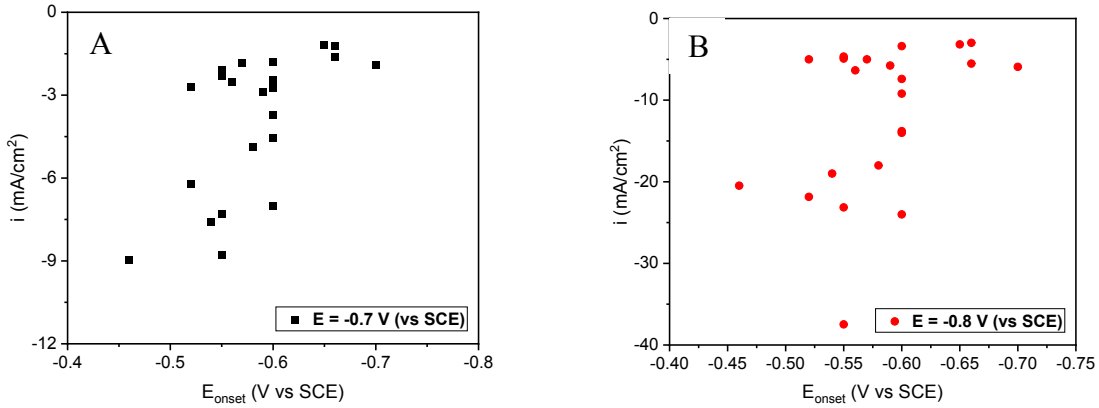

Figure S9. Current density vs onset potential at A) -0.7 V.B) -0.8 V.

Eq. S1-S6 were obtained using multivariate regressions and include the 2nd order terms to relate 3 synthesis conditions to each structural feature. The 2nd-order terms capture the interactions between features.

$$N_{Pyridinic} = 1.29 + 4.65 \times 10^{-3}\, Temperature - 0.183\, Heating\ rate - 0.403\, Hold\ time - 3.01 \times 10^{-6}\, T - 3.58 \times 10^{-4}\, Temperature \cdot Heating\ rate - 4.49 \times 10^{-4}\, Temperature \cdot Hold\ time + 0.0185 Heating\ rate^2 + 0.0248\, Heating\ rate \cdot Hold\ time + 0.0603\, Hold\ time^2$$

(Eq. S1)

$$N_{Pyrrolic} = 2.19 - 9.28 \times 10^{-3}\, Temperature - 0.155\, Heating\ rate - 0.192\, Hold\ time + 1.04 \times 10^{-5}\, T + 1.21 \times 10^{-4}\, Temperature \cdot Heating\ rate - 2.51 \times 10^{-4}\, Temperature \cdot Hold\ time + 0.0195\, Heating\ rate^2 - 0.0168\, Heating\ rate \cdot Hold\ time + 1.24 \times 10^{-3} Hold\ time^2$$

(Eq. S2)

$$N_{Graphitic} = -0.664 - 0.0123\, Temperature - 1.36 \times 10^{-3} Heating\ rate - 0.582\, Hold\ time + 1.70 \times 10^{-} - 9.52 \times 10^{-5}\, Temperature \cdot Heating\ rate + 2.68 \times 10^{-4}\, Temperature \cdot Hold\ time - 4.59 \times 10^{-3} Heating\ rate^2 + 0.0178\, Heating\ rate \cdot Hold\ time + 0.0503\, Hold\ time^2$$

(Eq. S3)

$$BET\ surface\ area = -53.9 + 3.51\, Temperature + 12.2\, Heating\ rate + 2.63\, Hold\ time - 4.40 \times 10^{-3}\, Tempera - 1.06 \times 10^{-3}\, Temperature \cdot Heating\ rate + 0.114\, Temperature \cdot Hold\ time - 2.72\, Heating\ rate^2 + 1.71\, Heating\ rate \cdot Hold\ time - 7.90\, Hold\ time^2$$

(Eq. S4)

$$Micropore\ volume = -0.0666 + 4.76 \times 10^{-4}\, Temperature + 0.0250\, Heating\ rate - 0.0143\, Hold\ time - 1.11 \times 10^{-6}\, Temperature^2 + 3.51 \times 10^{-5}\, Temperature \cdot Heating\ rate + 8.14 \times 10^{-5}\, Temperature \cdot Hold\ time - 3.84 \times 10^{-3}\, Heating\ rate^2 + 6.30 \times 10^{-4} Heating\ rate \cdot Hold\ time - 2.57 \times 10^{-3} Hold\ time^2$$

(Eq. S5)

$$\%\ crystallinity = 69.0 - 3.20 \times 10^{-4}\, Temperature + 3.74\, Heating\ rate + 0.193\, Hold\ time - 6.82 \times 10^{-5}\, Te + 2.44 \times 10^{-3}\, Temperature \cdot Heating\ rate + 5.23 \times 10^{-3}\, Temperature \cdot Hold\ time - 0.362\, Heating\ rate^2 - 0.107\, Heating\ rate \cdot Hold\ time - 0.133\, Hold\ time^2$$

(Eq. S6)

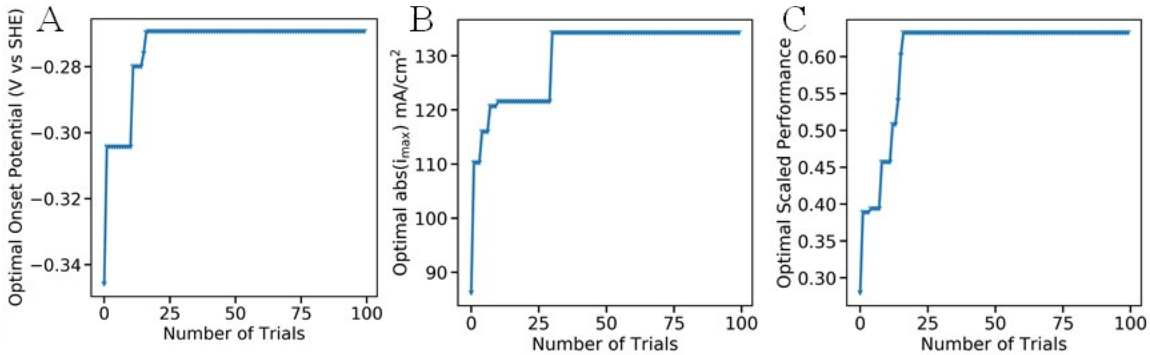

Figure S10. Learning curves for HER performance. The number of trials in Bayesian Optimization is plotted against A) optimal onset potential, B) maximum current density (absolute values), C) scaled performance calculated using Eq. S7, observed in the dataset.

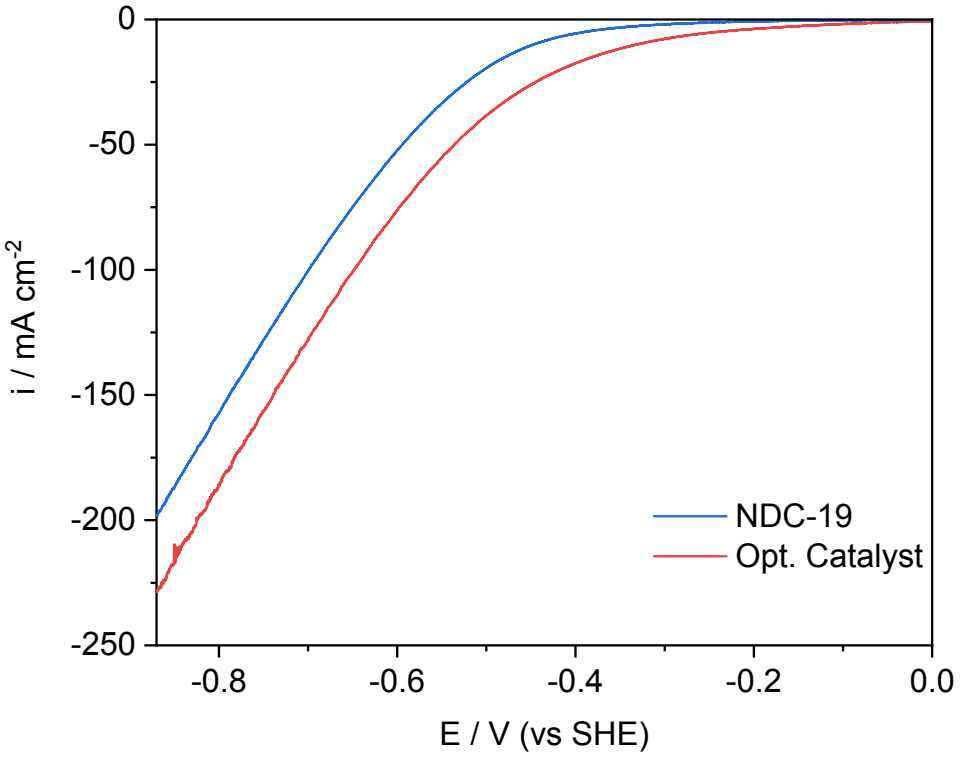

Figure S11. HER polarization curves of the optimal catalyst in the original set vs the optimal catalyst suggested from the multi-objective optimization and tested experimentally (scenario iii).

The parity plots and the accuracy of the regression models are shown in Figure S12 and S13.

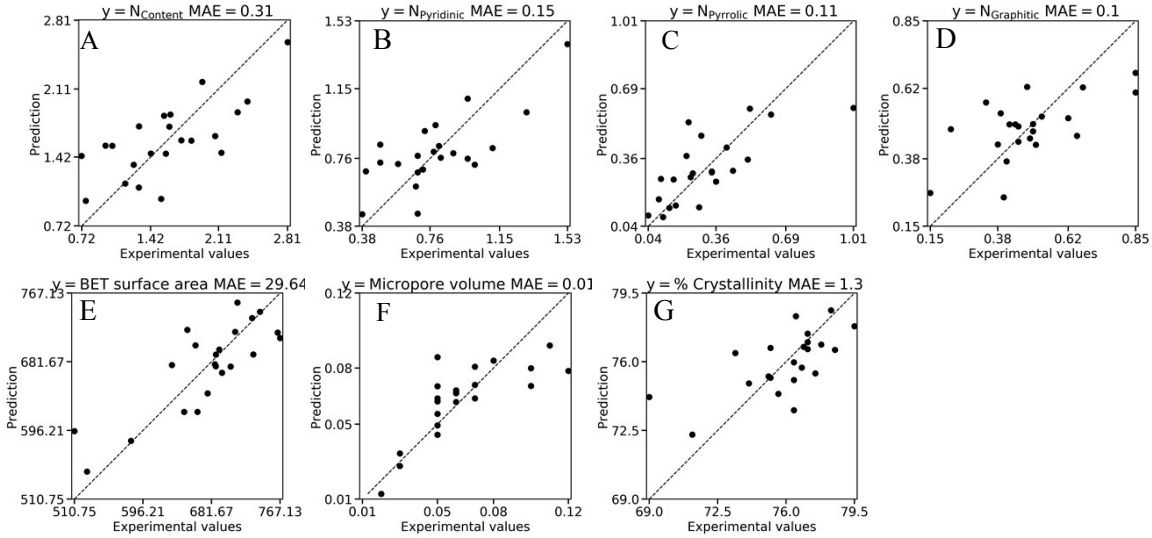

Figure S12. Parity plots of regression models relating structural features to synthesis conditions A)-G) correspond to Eq. 1 and Eq. S1-S6, respectively.

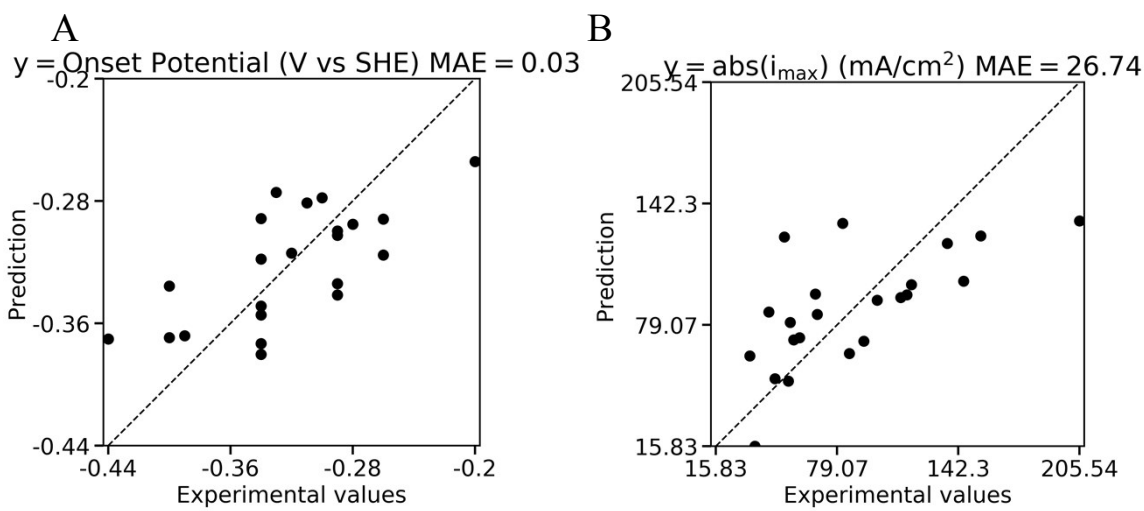

Figure S13. Parity plots of regression models relating HER performance to synthesis conditions.

$$Scaled\ Performance_i = 0.5\frac{onset\ potential_i - \min(onset\ potential)}{\max(onset\ potential) - min(onset\ potential)} + 0.5\frac{abs(i_{max})_i - \min(abs(i_{max}))}{\max(abs(i_{max})) - \min(abs(i_{max}))}$$

(Eq. S7)

Here i stands for ith NDC sample. A weight of 0.5 is used to ensure equal contributions from the both variables.

Table S4A. Optimum synthesis conditions for different scenarios.

	Optimum synthesis conditions		
	Final temp (^oC)	Heating rate (^oC/min)	Time (hr)
i. Optimize onset potential	300	6.55	6
ii. Optimize i_{max}	300	5.83	4.86
iii. Co-optimize onset and i_{max}	300	6.46	5.2
iv. Optimize N content	300	8	6

Table S4B. Optimum structural features for different scenarios. The structural features are predicted using Eq. S1-S6.

	Optimum structural features					
	$N_{Pyridinic}$	$N_{Pyrrolic}$	$N_{Graphitic}$	S_{BET} m^2/g	V_m cm^3/g	% Crystallinity
i. Optimize onset potential	1.22	0.48	0.61	569.93	0.037	78.06
ii. Optimize i_{max}	0.86	0.42	0.42	622.51	0.059	78.89
iii. Co-optimize onset and i_{max}	0.97	0.45	0.46	603.59	0.049	78.48
iv. Optimize N content	1.40	0.57	0.62	545	0.013	75.97

Table S4C. Optimum HER performance for different scenarios. The HER performances are predicted using Eq. S1-S6 and Eqs. 2-3.

	Optimum HER performance	
	Onset potential	abs(i_{max}) (mA/cm^2)
i. Optimize onset potential	-0.27	127.7
ii. Optimize i_{max}	-0.28	134.4
iii. Co-optimize onset and i_{max}	-0.28	133.6
iv. Optimize N content	-0.27	124.3

References

1 Y. Zheng, Y. Jiao, L. H. Li, T. Xing, Y. Chen, M. Jaroniec and S. Z. Qiao, *ACS Nano*, 2014, **8**, 5290–5296.

2 B. R. Sathe, X. Zou and T. Asefa, *Catal. Sci. Technol.*, 2014, **4**, 2023–2030.

3 H. Jiang, J. Gu, X. Zheng, M. Liu, X. Qiu, L. Wang, W. Li, Z. Chen, X. Ji and J. Li, *Energy Environ. Sci.*, 2019, **12**, 322–333.